

Imprints of the Ejecta-Companion Interaction in Type Ia Supernovae

Philip Boehner⁽¹⁾, Tomasz Plewa⁽¹⁾, & Norbert Langer⁽²⁾

(1) Department of Scientific Computing, Florida State University; (2) Bonn University, Bonn, Germany

Introduction

In the single-degenerate (SD) supernova scenario, a carbon-oxygen white dwarf stably accretes matter from a binary companion until it reaches the critical mass (Chandrasekhar limit) of about 1.4 solar masses. This condition ignites carbon in the core, allowing for a thermonuclear deflagration to propagate through the star and eventually cause a supernova. We explore the resulting interaction between the supernova ejecta and the non-degenerate companion and discuss the observable evidence indicative of this particular supernova scenario.

Model

For our SD supernova simulations, we use Proteus, a multi-dimensional hydrodynamic block-structured AMR code based on the FLASH code [1] architecture. To solve the Euler equations, we use the split piece-wise parabolic method [2] with a Helmholtz stellar equation of state [3]. Self-gravity is calculated using a multipole Poisson solver. A set of passively advected mass scalars are utilized in order to track the evolution of different nuclear species as well as to differentiate between the supernova ejecta and the stripped companion material over the course of the simulation.

We perform two-dimensional, cylindrical, axisymmetric simulations with 200 mesh points per companion radius and varying domain sizes. We use reflective boundary conditions on the axis of symmetry and outflow boundary conditions elsewhere.

In our study, we consider various binary systems due to the fact that it is not known what type of binaries produce Type Ia supernovae. One supernova model and six binary configurations with suitable companions are considered in our study. The SN Ia W7 [4] model is used to represent a Chandrasekhar explosion of a carbon-oxygen white dwarf, and we consider seven companion types: four main-sequence-like (MS) stars of different masses, one subgiant (SG) star, and two red giant (RG) stars of different masses. In representing these different companions, we note that the degenerate core of the red giant stars are represented as point masses with the remainder of the envelope surrounding this point mass, whereas the other companions are represented without a point mass.

Analysis Methods

In addition to simulating the interaction between W7 ejecta with the companion star, we use a number of analysis tools to interpret the results. We first require a method for determining the amount of mass stripped from the companion. This is important from an observational point of view and allows for model validation. At the final simulated time, the surface of the companion star has not yet stabilized, so we designate the contour around the companion star center (identified as the point with the highest density) where the total energy of the surrounding material sum to zero to be the future surface, since the material inside of the gravitational potential will remain bounded to the companion, and the material outside will not. We then determine the final mass of the companion integrating the mass within this.

Another quantity of interest allowing for testing against observations for our models is the angular distribution of column density values of the final simulated state. These column density calculations integrate the supernova ejecta along rays originating from the center of the companion star. The purpose of this analysis is to determine whether structural anomalies lie within the supernova remnant as a result of the supernova-companion interaction.

Results

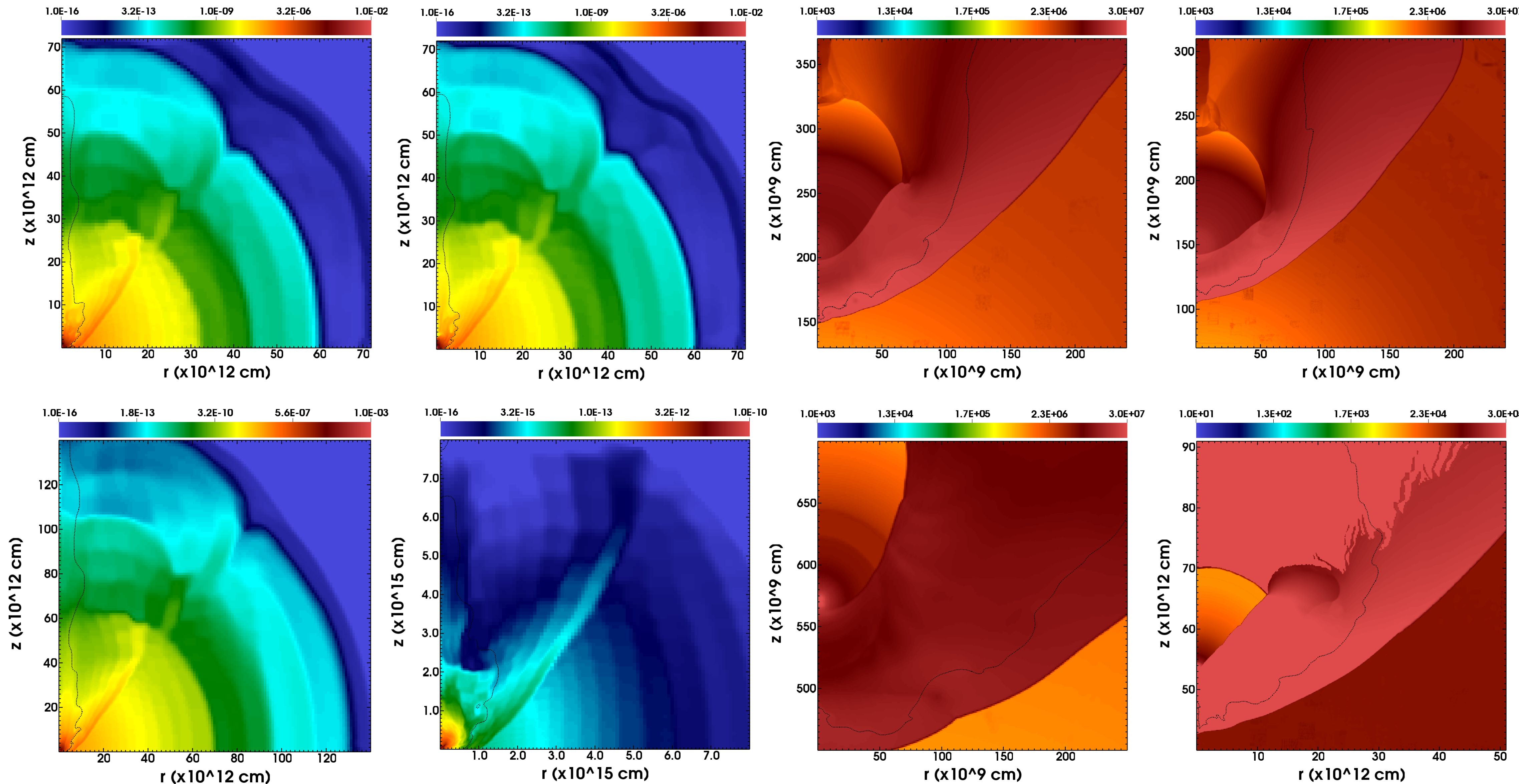


Fig. 1: Density distribution of four systems at the final simulated time (the final simulation times vary across each model). Top left: A small main-sequence companion designated MS38. Top right: The largest main-sequence companion MS54. Bottom left: The one subgiant companion SG. Bottom right: The largest red giant companion SY428. Note that the color scale changes in each panel in order to highlight important features of each supernova remnant, most importantly the existence of a low density region (or hole) resulting from the supernova ejecta interaction with the companion. The dotted contour line designates a 50/50 mix of companion material and supernova ejecta.

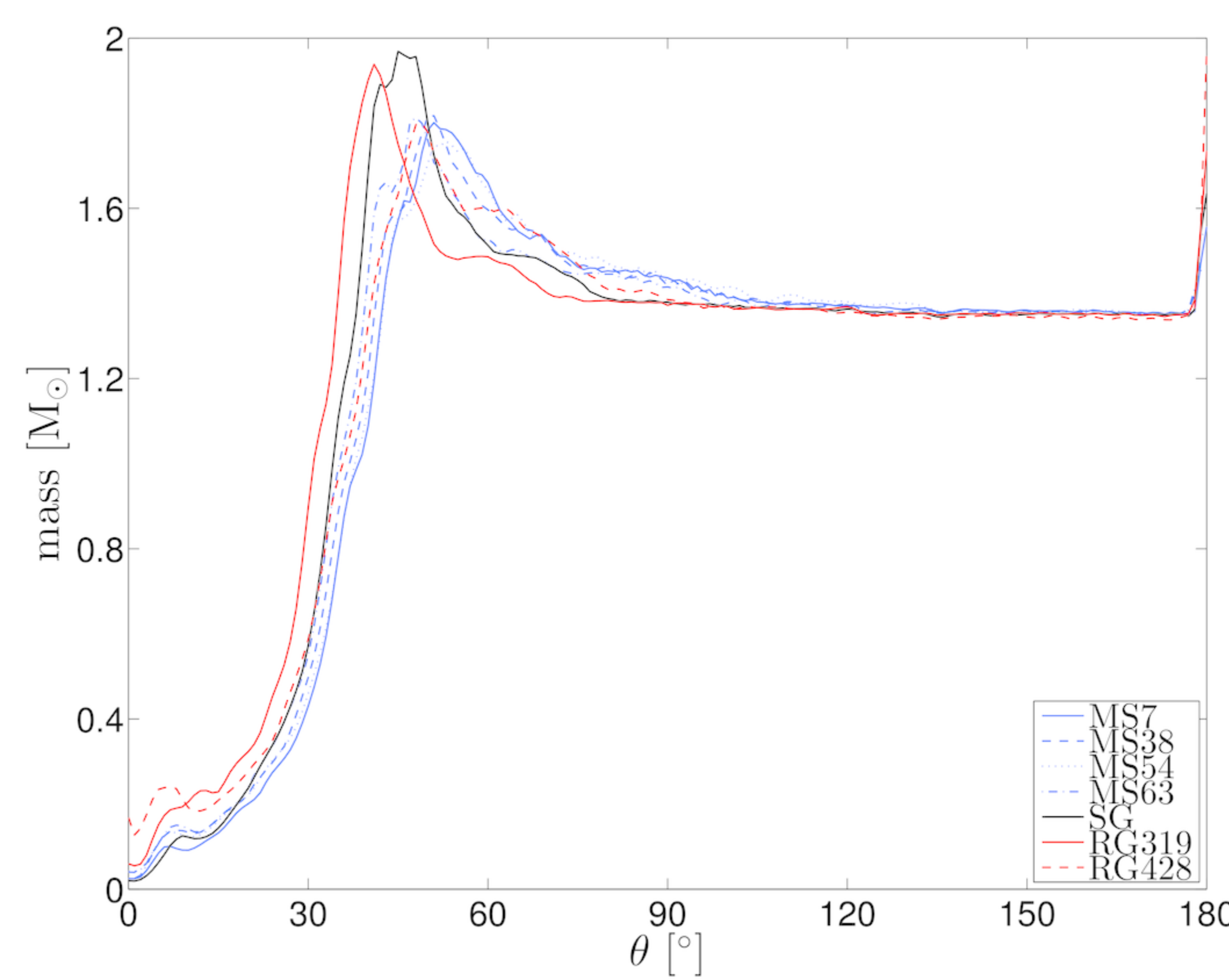


Fig. 2: Volume-integrated angular distribution of mass for all seven models. The mass is calculated by taking the column density value at a given angle and then integrating over the volume, yielding a mass of a sphere with constant density. This method is used instead of a simple column density method because the size of the domains differ, causing there to be substantially less mass per column in the red giant models (largest domains) that have been able to expand more than the main-sequence and subgiant models. Here 0 degrees corresponds to a column along the positive z-axis in Fig. 2 and 90 degrees corresponds to a column along the positive r-axis.

	Initial Mass (M_{\odot})	Final Mass (M_{\odot})	Stripped Mass (%)
MS7	1.53	1.16	24
MS38	1.15	0.90	22
MS54	1.24	0.93	25
MS63	1.13	0.89	21
SG	1.53	1.02	34
SY319	0.61	0.32	47
SY428	0.75	0.42	44

Table 1: Initial masses and final stripped masses for each companion. As expected, more evolved companions with more expanded (and thus weakly bound) envelopes experience more severe mass loss.

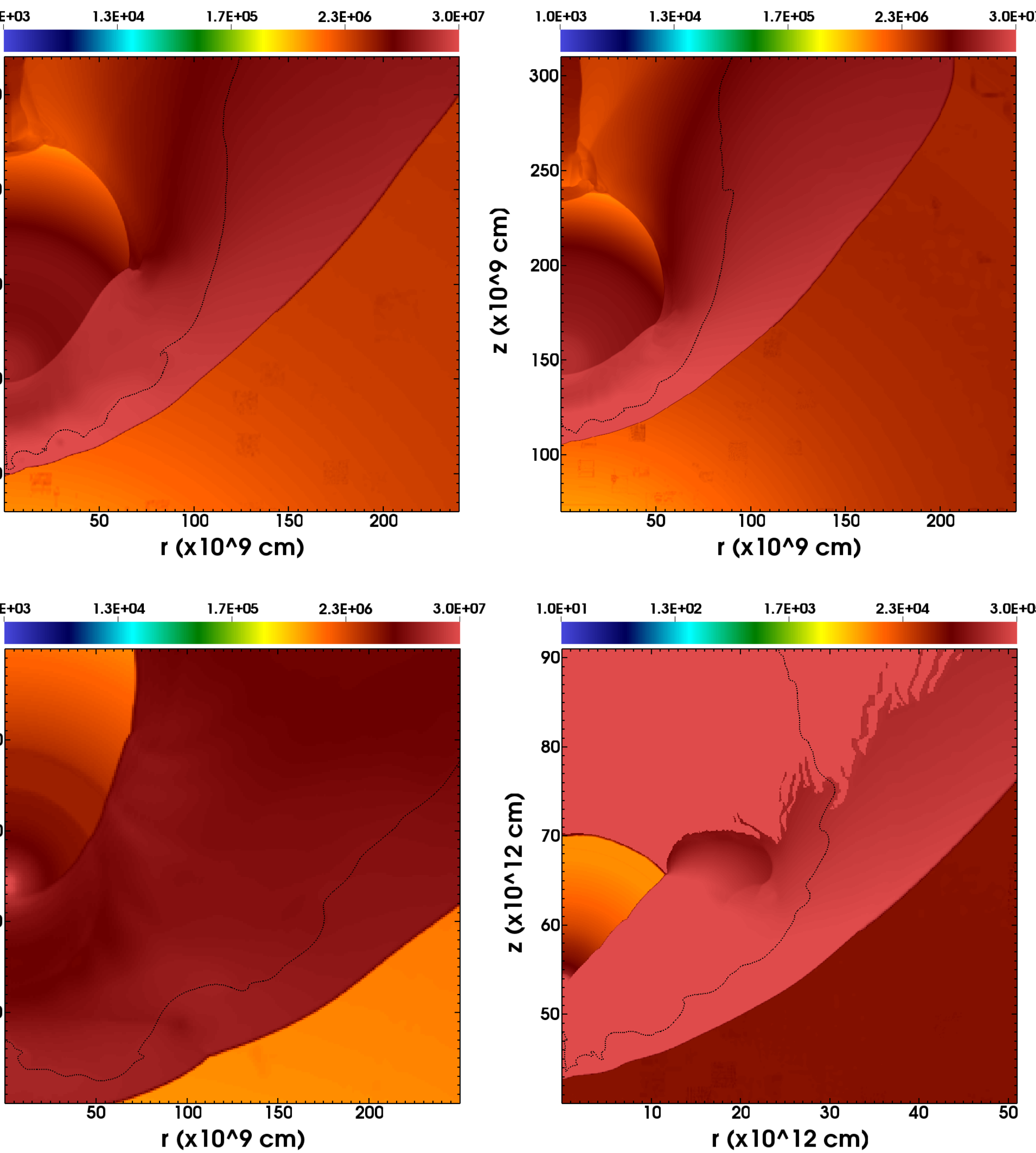


Fig. 3: Temperature distribution of the same four model binaries earlier in the simulation -- when the supernova shock has reached the core of the companion. Each image represents the respective binary systems shown in Fig. 1. Temperatures required for x-ray emission can occur within the shock-bounded region located between the transmitted shock and the bow shock. As the simulation progresses, this superheated material travels along the edge of the bow shock, potentially emitting x-rays through the evacuated hole, as opposed to these x-rays being absorbed by the rest of the supernova debris.

Discussion

In this study, our goal is to obtain model observables for the diverse types of binary systems that may produce Type Ia supernovae and in this way allow for testing one of the supernova formation channels. In Figure 1, the density distribution shows a bow-like structural feature bordering a low-density conical hole found in each model at their respective final times. The column density calculations in Figure 2 show this absence of material more clearly at the lower angles, and we find that regardless of the mass of the companion (for the models considered), the variation in the angular size of the hole is minimal.

We are also interested in determining the properties of the remaining companion star long after the supernova event. Table 1 shows the percentage of mass stripped from each of the companions at the end of the simulations. The evolved companions (the SG and SY models) have expanded, weakly bound envelopes, which results in more severe mass loss. This result could aid observers in determining whether stars in the vicinity of the center of a supernova remnant may be possible companion candidates, since our column density calculations show that the angular size of the hole is independent of the mass of the companion.

X-ray emission may result from the SN-companion interaction (Figure 3). In this preliminary study, we explore whether x-ray temperatures can even be reached at the most energetic point in the simulation. At this time, the superheated material is trapped between the companion and the supernova and is thus unobservable. As the material travels along the bow shock it will become observable, but in the process will also lose energy. However, we do find that at the most energetic time, the temperatures in this region allow for soft x-ray emission (0.1 to 5 KeV) across each companion type, with the main-sequence companions showing the most energetic x-ray emission (2.73 to 4.32 KeV for MS38), followed by the subgiant (1.08 to 2.43 KeV for SG) and then red giant companions (0.09 to 0.27 KeV for SY319).

References

- [1] Fryxell, B. et. al. 2000, ApJS, 131, 273
- [2] Colella, P., & Woodward, P.R. 1984, J. Comput. Phys., 54, 174
- [3] Timmes, F. X., & Swesty, F. D. 2000, ApJS 126, 501
- [4] Nomoto et al. 1984, ApJ, 286, 644
- [5] Norbert Langer - Private Communication, 2007